

# Vergasovaite $\text{Cu}_3\text{O}[(\text{Mo},\text{S})\text{O}_4][\text{SO}_4]$ , a new copper-oxy-molybdate-sulfate from Kamchatka

Autor(en): **Bykova, Elena Y. / Berlepsch, Peter / Kartashov, Pavel M.**

Objektyp: **Article**

Zeitschrift: **Schweizerische mineralogische und petrographische Mitteilungen  
= Bulletin suisse de minéralogie et pétrographie**

Band (Jahr): **78 (1998)**

Heft 3

PDF erstellt am: **06.08.2024**

Persistenter Link: <https://doi.org/10.5169/seals-59302>

## **Nutzungsbedingungen**

Die ETH-Bibliothek ist Anbieterin der digitalisierten Zeitschriften. Sie besitzt keine Urheberrechte an den Inhalten der Zeitschriften. Die Rechte liegen in der Regel bei den Herausgebern. Die auf der Plattform e-periodica veröffentlichten Dokumente stehen für nicht-kommerzielle Zwecke in Lehre und Forschung sowie für die private Nutzung frei zur Verfügung. Einzelne Dateien oder Ausdrucke aus diesem Angebot können zusammen mit diesen Nutzungsbedingungen und den korrekten Herkunftsbezeichnungen weitergegeben werden. Das Veröffentlichen von Bildern in Print- und Online-Publikationen ist nur mit vorheriger Genehmigung der Rechteinhaber erlaubt. Die systematische Speicherung von Teilen des elektronischen Angebots auf anderen Servern bedarf ebenfalls des schriftlichen Einverständnisses der Rechteinhaber.

## **Haftungsausschluss**

Alle Angaben erfolgen ohne Gewähr für Vollständigkeit oder Richtigkeit. Es wird keine Haftung übernommen für Schäden durch die Verwendung von Informationen aus diesem Online-Angebot oder durch das Fehlen von Informationen. Dies gilt auch für Inhalte Dritter, die über dieses Angebot zugänglich sind.

## Vergasovaite $\text{Cu}_3\text{O}[(\text{Mo,S})\text{O}_4][\text{SO}_4]$ , a new copper-oxy-molybdate-sulfate from Kamchatka

by Elena Y. Bykova<sup>1</sup>, Peter Berlepsch<sup>2</sup>, Pavel M. Kartashov<sup>1</sup>, Joël Brugger<sup>3</sup>, Thomas Armbruster<sup>4</sup> and Alan J. Criddle<sup>5</sup>

### Abstract

Vergasovaite occurs on encrustations of sulfates in fumaroles in the Northern part of the central fumarole field of cone II of the Northern Break of the Large Tolbachik Fissure Eruption (LTFE) on the Kamchatka peninsula. It is associated with chalcocyanite, dolerophanite, euchlorine, fedotovite, tenorite, Cu-bearing anglesite and native gold. Vergasovaite has an ideal formula  $\text{Cu}_3\text{O}[(\text{Mo,S})\text{O}_4][\text{SO}_4]$ . Its space group is *Pnma* with  $a = 7.420(3)$ ,  $b = 6.741(2)$ ,  $c = 13.548(5)$  Å,  $V = 677.6(2)$  Å<sup>3</sup>, and  $Z = 4$ . The five strongest lines  $d_{\text{calc}}$  [Å] ( $I_{\text{calc}}$ ,  $hkl$ ) in the X-ray powder pattern are: 3.096 (100, 104); 3.377 (69, 020); 2.998 (56, 121); 2.498 (54, 220); and 3.580 (37, 201). The olive-green mineral is transparent and distinctly pleochroic from olive-green to a yellowish to brownish-green. Microprobe analyses revealed a partial substitution of Mo by S and minor V, leading to the empirical formula  $(\text{Cu}_{2.82(7)}, \text{Zn}_{0.10(7)}, \text{Pb}_{0.01(1)})_{\Sigma = 2.92(9)}\text{O}[(\text{Mo}_{0.79(7)}, \text{S}_{0.20(5)}, \text{V}_{0.04(3)})_{\Sigma = 1.04(3)}\text{O}_4][\text{SO}_4]$ . IR spectroscopy showed vergasovaite to be free of H<sub>2</sub>O and OH thus the mineral is a fully oxidized mixed copper-oxy-molybdate-sulfate. Vergasovaite is isostructural with synthetic  $\text{Cu}_3\text{O}[\text{MoO}_4]_2$ .

**Keywords:** vergasovaite, new mineral, molybdate, sulfate, exhalate, Kamchatka.

### Introduction

The occurrence of Mo-minerals on volcanoes is very rare. The most common species are molybdenite  $\text{MoS}_2$ , e.g., from the Merapi volcano on Central Java, Indonesia (KAVALIERIS, 1994), at Mount St. Helens, Washington, USA (BERNARD and LE GUERN, 1986), or from Mount Vesuvius (ZAMBONINI, 1935), and ilsemanite  $\text{Mo}_3\text{O}_8 \cdot 5\text{H}_2\text{O}$  (BERNARD and LE GUERN, 1986; BERNARD et al., 1990). A uniquely rich association of Mo-minerals was found in the high temperature exhalates of Kudrjavyi volcano (Iturup, Kuril Islands) where Re-rich and Re-free molybdenite, powellite  $\text{Ca}[\text{MoO}_4]$ , molybdoscheelite  $\text{Ca}[(\text{W},\text{Mo})\text{O}_4]$ , tugarinovite  $\text{MoO}_2$ , molybdite  $\text{MoO}_3$ , and ilsemanite were identified (BYKOVA et al., 1995). The

new mixed copper-oxy-molybdate-sulfate described here occurs in fumarolic products of the Large Tolbachik Fissure Eruption (LTFE) on the Kamchatka peninsula (Fig. 1a).

The LTFE is located in the Southern part of the Kliuchevskaya group of volcanoes in central Kamchatka, where the most active volcanoes of the Kurile-Kamchatka region are located. The Kliuchevskaya group of volcanoes consists of three active (Kliuchevskoi, Bezymianny, and Plosky Tolbachik) and some inactive volcanoes (Fig. 1b). The eruptive zone extends linearly over 30 km. As a consequence of enormous lava extrusions, the top of Plosky Tolbachik collapsed, thus forming a caldera with a diameter of 1.7 km and a depth of more than 400 m.

The LTFE has been a source of exhalative

<sup>1</sup> Institute for Geology of Ore Deposits of the Russian Academy of Science, IGEM RAN, Staromonetny per. 35-303, 109017 Moscow, Russia.

<sup>2</sup> Mineralogisch-Petrographisches Institut, Universität Basel, Bernoullistrasse 30, CH-4056 Basel, Switzerland. <berlepsch@ubaclu.unibas.ch> (corresponding author)

<sup>3</sup> VIEPS, Department of Earth Sciences, Monash University, Clayton, Victoria 3168, Australia.

<sup>4</sup> Laboratorium für Chemische und Mineralogische Kristallographie, Universität Bern, Freiestrasse 3, CH-3012 Bern, Switzerland.

<sup>5</sup> Department of Mineralogy, The Natural History Museum, Cromwell Road, UK-London SW7 5BD, England.

minerals of unique diversity and abundance, the formation of which was favored by magma saturated with gases and originating at large depth and escaping at high velocity. Up to now, more than 120 minerals have been found from the

LTFE (VERGASOVA and FILATOV, 1993) of which 16 are new species. The central fumarole field, located near the top of the crater of the second cone of the Northern Break (Fig. 1c), is of most interest because of its high exhalative activity. Besides

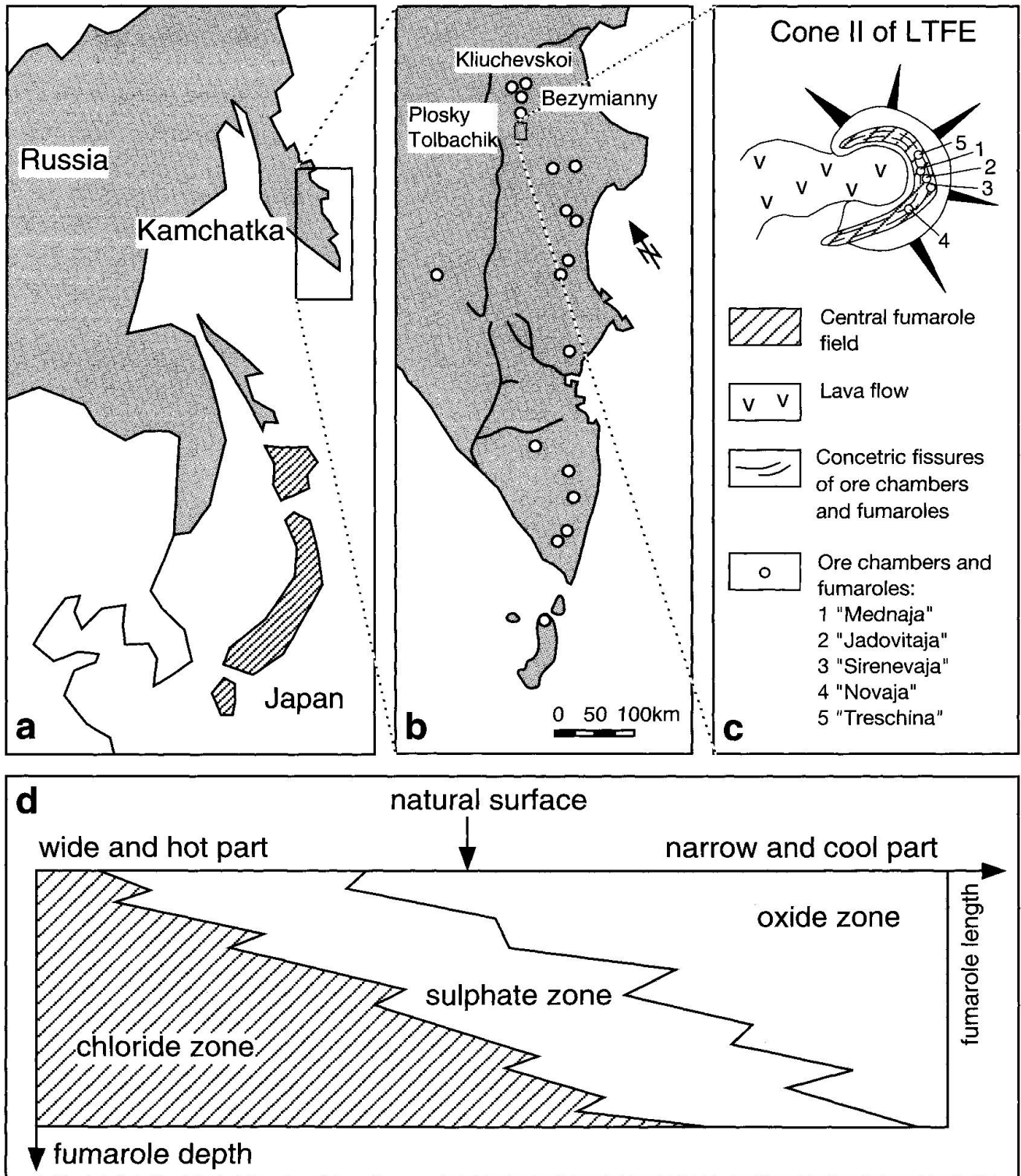


Fig. 1 Occurrence of vergasovaite: (a) Kamchatka; (b) some active volcanoes, calderas, and craters including the Kliuchevskaya group of volcanoes (modified after BRAITSEVA et al., 1995); (c) schematic map of cone II of the LTFE south of Plosky Tolbachik with the central fumarole field; (d) schematic cross section through "Treschina" fumarole.

Tab. 1 Optical and other physical properties of vergasovaite.

|                                    |   |
|------------------------------------|---|
| Morphology                         | short prismatic   |
| Forms                              | pinacoid: {010}   |
|                                    | prisms: {110} {120} {130}   |
|                                    | bipyramids: {111} {263} {315}                                       |
| Colour (megascopic)                | olive-green   |
| Streak                             | light-yellow  |
| Lustre                             | vitreous  |
| Fluorescence                       | not observed  |
| Hardness (VHN <sub>25g</sub> )     | mean of 6: 357 g/cm <sup>3</sup> (range 302–413 g/cm <sup>3</sup> ) |
| Hardness (Mohs)                    | 4–5, 5–5.5 on face subparallel (010)                                |
| Cleavage                           | not observed  |
| Parting                            | not observed  |
| Tenacity                           | brittle   |
| Fracture                           | uneven  |
| Density                            | 4.32 g/cm <sup>3</sup> (calculated)                                 |
| Ore microscopy                     |   |
| Colour                             | grey  |
| Internal reflections               | ubiquitous, light green to colourless                               |
| Anisotropy                         | masked by internal reflections                                      |
| Birefractance                      | measurable but discernible  |
| Pleochroism (transmitted light)    | olive-green to yellowish/brownish-green                             |
| Pleochroism (reflected light)      | absent  |
| Standard used                      | SiC   |
| n <sub>calc</sub> (589 nm)         | 1.87–1.98 (average 1.925)   |
| n <sub>calc</sub> (Gladstone-Dale) | 1.819   |
| Mandarino Compatibility Index      | poor  |

high temperature Zn–Pb–Cu-compounds, the mineral forming elements are Fe, As, P, Bi, Te, Rb, Cr, Se, V, Au, and Mo.

The name for the new mineral was chosen to honour Lidia Pavlovna Vergasova, born 1941, in recognition of her contribution to the mineralogy of volcanic exhalates of Kamchatka in general, and the mineralogy of the Tolbachik region in particular. She described from there many new minerals including alarsite, alumoklyuchevskite, fedotovite, georgbokiite, ilinskite, kamchatkite, klyuchevskite, leningradite, lesukite, piypite, ponomarevite, sophiite, tolbachite, vlodavetsite.

The mineral and the name were approved (proposal 98-009) by the Commission on New Mineral and Mineral Names (CNMMN) of the International Mineralogical Association (IMA). Type Material is deposited at the Fersman Mineralogical Museum in Moscow (No. 2328/1) and at the Naturhistorisches Museum in Basel.

### Occurrence and genetic environment

Vergasovaite was found in 1993 in a fumarole called "Treschina" (Russian for fissure) in the Northern part of the central fumarole field of cone II of the Northern Break of the LTFE on

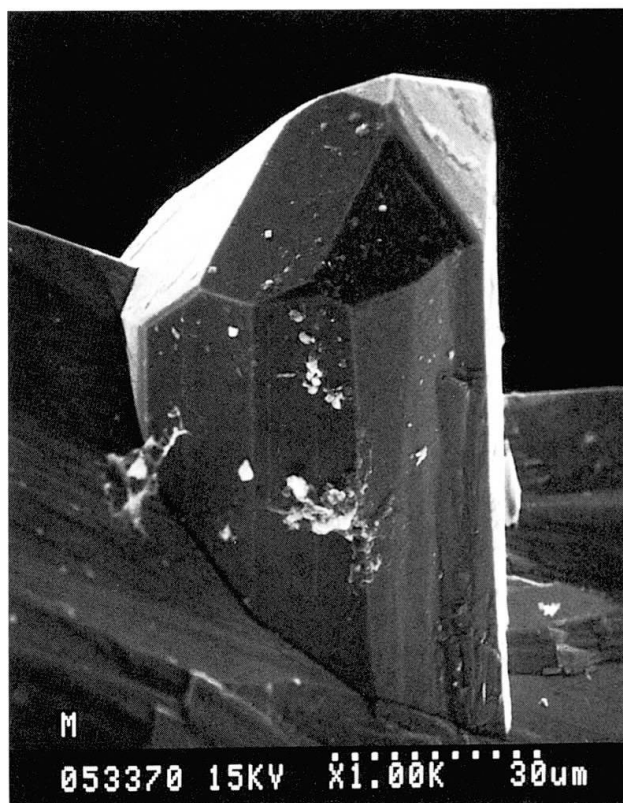


Fig. 2 SEM-image of a small and form-rich vergasovaite crystal that grew on a larger crystal displaying simpler forms.

Tab. 2 Vergasovaite measurements on optical goniometer (angles in degrees).

| Face                        | Form            | Size   | $\varphi_{\text{obs}}$ | $\rho_{\text{obs}}$ | $\varphi_{\text{calc}}$ | $\rho_{\text{calc}}$ |
|-----------------------------|-----------------|--------|------------------------|---------------------|-------------------------|----------------------|
| (010)                       | Pinacoid {010}  | medium | 359.2                  | 90.7                | 360                     | 90                   |
| (110)                       | Prism {110}     | small  | 238.0                  | 90                  | 241.4                   | 90                   |
| (120)                       | Prism {120}     | small  | 40.1                   | 90                  | 42.5                    | 90                   |
| (130)                       | Prism {130}     | large  | 31.2                   | 90                  | 31.4                    | 90                   |
| ( $\bar{1}30$ )             | "               | large  | 148.8                  | 89.8                | 148.6                   | 90                   |
| ( $\bar{1}\bar{3}0$ )       | "               | medium | 329.2                  | 90                  | 328.6                   | 90                   |
| (111)                       | Bipyramid {111} | large  | 59.7                   | 46.4                | 61.4                    | 46.0                 |
| ( $\bar{1}\bar{1}\bar{1}$ ) | "               | small  | 301.8                  | 49.1                | 298.6                   | 46.0                 |
| ( $\bar{1}\bar{1}1$ )       | "               | large  | 116.0                  | 46.6                | 118.6                   | 46.0                 |
| (263)                       | Bipyramid {263} | medium | 33.2                   | 50.0                | 31.4                    | 49.3                 |
| ( $\bar{3}15$ )             | Bipyramid {315} | small  | 279.8                  | 28.2                | 280.3                   | 29.0                 |
| ( $\bar{3}\bar{1}\bar{5}$ ) | "               | medium | 259.0                  | 28.0                | 259.7                   | 29.0                 |

The measured angles were centered for the (111) and ( $\bar{1}\bar{1}1$ ) faces. With the orientation  $b > a > c$  of the crystal lattice (according to the rules of DONNAY and ONDIK, 1973) the axial ratios are:  
 $a_0 : 1 : c_0 = 0.546 : 1 : 0.497$  (X-ray)  
 $a_0 : 1 : c_0 = 0.535 : 1 : 0.497$  (goniometer)

Kamchatka peninsula (FEDOTOV and MARKHININ, 1984). Treschina is a wedge-shaped fumarole with a temperature gradient that decreases from the wide to the narrow part (Fig. 1d). This gradient is a function of the width of the fumarole which controls the speed with which the gases escape to the atmosphere and has led to a mineralogical zonation within the fumarole. From the widest and hottest part within the chloride zone, through the sulfate zone to the narrowest and coolest part within the oxide zone, the sequence of representative minerals is: tolbachite  $\text{CuCl}_2$ , chalcocyanite  $\text{Cu}[\text{SO}_4]$ , and tenorite  $\text{CuO}$ .

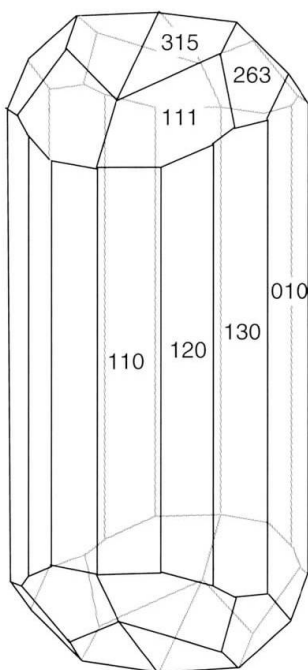


Fig. 3 Idealized SHAPE-drawing of vergasovaite.

The new mineral occurred on a sulfate encrustation extracted from the sulfate zone, approximately 20 cm below surface, where it formed directly from fumarolic gases by sublimation. The temperature of the gases in the sulfate zone is 150–170 °C. The composition of the gases is as following (approximate values): 80%  $\text{H}_2\text{O}$ ; 12%  $\text{N}_2$ ; 4%  $\text{CO}_2$ ; 2%  $\text{H}_2$ ; 0.5–0.1%  $\text{HCl} > \text{CH}_4 > \text{CO}$ ;  $< 0.1\% \text{H}_2\text{S} > \text{NH}_3 > \text{O}_2 > \text{F}_2$  (personal comment S.F. Glavatskiy).

Associated minerals are chalcocyanite  $\text{Cu}[\text{SO}_4]$ , dolerophanite  $\text{Cu}_2\text{O}[\text{SO}_4]$ , euchlorine  $\text{NaKC}_3\text{O}[\text{SO}_4]_3$ , fedotovite  $\text{K}_2\text{Cu}_3\text{O}[\text{SO}_4]_3$ , tenorite  $\text{CuO}$ , Cu-bearing anglesite  $\text{Pb}[\text{SO}_4]$  and native gold. Vergasovaite grows directly on chalcocyanite and dolerophanite crystal surfaces where it was formed after chalcocyanite and before tenorite.

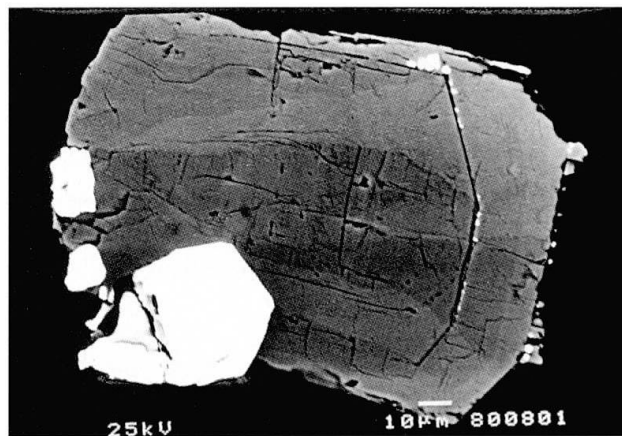


Fig. 4 BSE-image of vergasovaite: the white inclusions are Cu-bearing anglesite. Sector and oscillatory zonations are visible.



Tab. 3 Reflectance data for vergasovaite measured in air (SiC standard).

| $\lambda$ (nm) | R1    | R2    |
|----------------|-------|-------|
| 400            | 10.64 | 13.03 |
| 420            | 10.39 | 12.62 |
| 440            | 10.16 | 12.17 |
| 460            | 9.95  | 11.86 |
| 470            | 9.85  | 11.69 |
| 480            | 9.8   | 11.61 |
| 500            | 9.66  | 11.4  |
| 520            | 9.55  | 11.22 |
| 540            | 9.42  | 11.06 |
| 546            | 9.4   | 11.01 |
| 560            | 9.35  | 10.93 |
| 580            | 9.26  | 10.78 |
| 589            | 9.22  | 10.76 |
| 600            | 9.16  | 10.68 |
| 620            | 9.11  | 10.63 |
| 640            | 9.07  | 10.52 |
| 650            | 9     | 10.48 |
| 660            | 9.03  | 10.47 |
| 680            | 9     | 10.42 |
| 700            | 9.03  | 10.45 |

### Optical and other physical properties

The optical and other physical properties of vergasovaite are summarized in table 1. Rare single crystals are flattened, shortened prisms, slightly elongated parallel the *c*-axis and do not exceed 0.3 mm in size. Single crystals are frequently intergrown (Fig. 2), sometimes forming radiating aggregates up to 0.6 mm overgrowing the matrix. The crystal used for the structure determination was also studied using an optical goniometer. The measured forms (Tab. 2) are: a pinacoid {100}; three prisms: {110} {120} {130}; and three bipyramids: {111} {263} {315}. It seems as if the larger crystals display a reduced variety of forms, with the pinacoid and prisms dominating, compared to the smaller crystals. Presumably the latter grew slower and later than the large crystals. Twinning was not observed. An drawing of ideal vergasovaite is shown in figure 3.

Vergasovaite is transparent and has a megascopic olive-green colour. The streak is light-yellow, the lustre is vitreous and no fluorescence was observed. Micro-indentations were done with a load of 25 g on a LEITZ Durimet 2 microhardness tester. Six perfect, slightly fractured indentations on randomly oriented polished surfaces of three grains give a mean VHN of 357 kg/mm<sup>2</sup> with a range of 302–413 kg/mm<sup>2</sup> which corresponds to a Mohs' hardness of 4–5. Measurements perpendicular to a face subparallel to (010) yielded a Mohs' hardness of 5–5.5 (personal comment D.K. Cherbachev).

Tab. 4 Powder data for vergasovaite obtained with a Gandolfi camera (114.5 mm diameter, FeK<sub>α</sub> X-radiation). Intensities were visually estimated.

| $I_{est}^1$ | $d_{meas}$ | $d_{calc}^2$ | $I_{calc}^2$ | hkl <sup>2,3</sup> |
|-------------|------------|--------------|--------------|--------------------|
| 30          | 3.71       | 3.71         | 33           | 2 0 0              |
| 10          | 3.580      | 3.580        | 37           | 2 0 1              |
| 60          | 3.391      | 3.377        | 69           | 0 2 0              |
| 60          | 3.342      | 3.360        | 24           | 1 1 3              |
| 30          | 3.226      | { 3.258      | 12           | 2 0 2              |
|             |            | { 3.252      | 32           | 2 1 0              |
| 100         | 3.077      | 3.096        | 100          | 1 0 4              |
| 30          | 2.990      | 2.998        | 56           | 1 2 1              |
| 60          | 2.542      | { 2.558      | 27           | 1 0 5              |
|             |            | { 2.546      | 12           | 1 2 3              |
| 60          | 2.500      | 2.498        | 54           | 2 2 0              |
| 30          | 2.400      | { 2.434      | 9            | 3 0 1              |
|             |            | { 2.398      | 15           | 0 2 4              |
| 10          | 2.381      | 2.392        | 2            | 1 1 5              |
| 60          | 2.275      | 2.282        | 31           | 1 2 4              |
| 30          | 2.167      | 2.171        | 33           | 1 0 6              |
| 10          | 2.126      | 2.128        | 11           | 1 3 1              |
| 10          | 2.057      | 2.067        | 4            | 1 1 6              |
| 10          | 1.903      | 1.906        | 3            | 2 3 1              |
| 10          | 1.849      | 1.852        | 5            | 2 3 2              |
| 10          | 1.764      | 1.768        | 7            | 3 1 5              |
| 10          | 1.715      | 1.7175       | 5            | 4 0 3              |
| 10          | 1.678      | { 1.6885     | 28           | 0 4 0              |
|             |            | { 1.6801     | 15           | 2 2 6              |
| 30          | 1.606      | 1.6100       | 9            | 3 2 5              |
| 5           | 1.582      | 1.5816       | 18           | 4 2 2              |
| 10          | 1.544      | 1.5478       | 16           | 2 0 8              |
| 10          | 1.534      | 1.5368       | 2            | 2 4 0              |
| 10          | 1.518      | 1.5206       | 10           | 0 2 8              |
| 10          | 1.389      | 1.3934       | 11           | 3 2 7              |
| 10          | 1.387      | { 1.3810     | 4            | 5 1 3              |
|             |            | { 1.3734     | 5            | 3 1 8              |

<sup>1</sup> Intensities assigned by visual estimate.

<sup>2</sup> Calculated on the basis of the structural data published by BERLEPSCH et al. (in press) by the program LAZY PULVERIX (YVON et al., 1977) for neutral Cu, Mo, S and O.

<sup>3</sup> Indices were chosen using the calculated intensities.

Using the empirical formula derived from electron microprobe analysis (Tab. 7) and the single-crystal (CAD4 data) cell parameters (Tab. 5), the calculated density of vergasovaite was determined to be 4.32 g/cm<sup>3</sup>. The density could not be measured because grains of suitable size contain inclusions of Cu-bearing anglesite (Fig. 4) and sink in the Clerici liquid.

Vergasovaite has high refractive indices (> 1.9), thus it was treated as an ore mineral in obtaining its optical data (the mineral reacts with phosphorous immersion liquids and dissolves in selenium-sulfur melts). Under plane polars the colour is grey with ubiquitous internal reflections

Tab. 5 Cell parameters of vergasovaite.

|                            | CAD4 data <sup>1</sup> | Powder data <sup>1,2</sup> |
|----------------------------|------------------------|----------------------------|
| Crystal system             | orthorhombic           | orthorhombic               |
| Space group                | <i>Pnma</i>            | <i>Pnma</i>                |
| <i>a</i> [Å]               | 7.406(1)               | 7.420(3)                   |
| <i>b</i> [Å]               | 6.739(2)               | 6.741(2)                   |
| <i>c</i> [Å]               | 13.573(2)              | 13.548(5)                  |
| <i>V</i> [Å <sup>3</sup> ] | 677.4(2)               | 677.6(2)                   |
| <i>Z</i>                   | 4                      | 4                          |

<sup>1</sup> Orientation *c* > *a* > *b* according to BERLEPSCH et al. (in press) which corresponds to the standard space group setting *Pnma*.

<sup>2</sup> Cell parameters were obtained by a least squares refinement performed with the program from APPLEMAN and EVANS (1973).

which are light green to colourless. Internal reflections mask the anisotropy and the birefractance is measurable but not discernible. Pleochroism in transmitted light changes from olive-green (parallel to the morphological elongation) to a yellowish to brownish green (perpendicular to the morphological elongation). Pleochroism in reflected light is absent.

The refractive indices calculated from the reflectance values at 589 nm (and assuming *k* = 0) are 1.87–1.98 (average 1.925). The measurements were made on the best of three crystals, but we cannot be sure that the constants (*R* and *n*) represent extreme values for the species, nor that the average corresponds to the mean. The reflectance values are listed in table 3.

The mean *n*<sub>calc</sub> obtained from the Gladstone-Dale relationship (MANDARINO, 1979) and using the chemical data given in table 7, the revised Gladstone-Dale constants in MANDARINO (1981), and the calculated density (4.32 g/cm<sup>3</sup>) is 1.819. The Mandarino Compatibility Index is poor which can be explained by the reasons given above as well as the unreliability of the Gladstone-Dale constants, especially for MoO<sub>3</sub>.

The X-ray powder diffraction pattern was obtained with a Gandolfi camera (114.5 mm diameter) using Mn-filtered FeK<sub>α</sub> X-radiation (*λ* = 1.93728 Å). The X-ray powder diffraction data for vergasovaite are listed in table 4. Relative intensities of the reflections were assigned by visual estimate. In table 5 the unit-cell parameters obtained from CAD4 and powder data are listed. Considering the range of Mo <-> S substitution, the agreement between the two cell parameter sets is excellent.

Tab. 6 Interpretation of the absorption bands in the IR-spectrum (Fig. 5) of vergasovaite.

| Peaks [cm <sup>-1</sup> ]    | Bond type | Vibration type |
|------------------------------|-----------|----------------|
| 462, 480                     | Mo–O      | bending        |
| 533, 602                     | Cu–O      | stretching     |
| 624, 637, 670, 690           | S–O       | bending        |
| 817, 882, 928, 963           | Mo–O      | stretching     |
| 1012, 1086, 1130, 1150, 1200 | S–O       | stretching     |

### Chemical composition

About 1 mg of vergasovaite was mixed with 150 mg KBr and pressed to a 10 mm diameter pellet. The IR-spectrum was measured from 400–4000 cm<sup>-1</sup> against pure KBr on a SPECORD 75 IR-spectrometer. The results showed vergasovaite to be free of H<sub>2</sub>O or OH (Fig. 5). The interpretation of the absorption bands is given in table 6.

The results of the chemical analyses are summarized in table 7. 18 analyses were performed on one crystal with a CAMEBAX SX-50 EMP operated at 20 kV, 30 nA, and a spot-size beam. The main elements measured were Cu, Mo, and S, and the minor constituents are Zn, V and Pb. BERLEPSCH et al. (in press) also found independently FeO ≤ 0.09, TiO<sub>2</sub> ≤ 0.06, TeO<sub>2</sub> ≤ 0.16 wt% and by using WDS scans, no additional element with atomic number ≥ 10 was detected.

The empirical formula (on the basis of nine oxygens p.f.u., and the mean of 18 analyses on one grain) is (Cu<sub>2.82(7)</sub>Zn<sub>0.10(7)</sub>Pb<sub>0.01(1)</sub>)<sub>Σ = 2.92(9)</sub> O[(Mo<sub>0.79(7)</sub>S<sub>0.20(5)</sub>V<sub>0.04(3)</sub>)<sub>Σ = 1.04(3)</sub>O<sub>4</sub>][SO<sub>4</sub>] and matches very well with the formula Cu<sub>3</sub>O[(Mo<sub>0.742(7)</sub>S<sub>0.258(7)</sub>O<sub>4</sub>][SO<sub>4</sub>] obtained from the

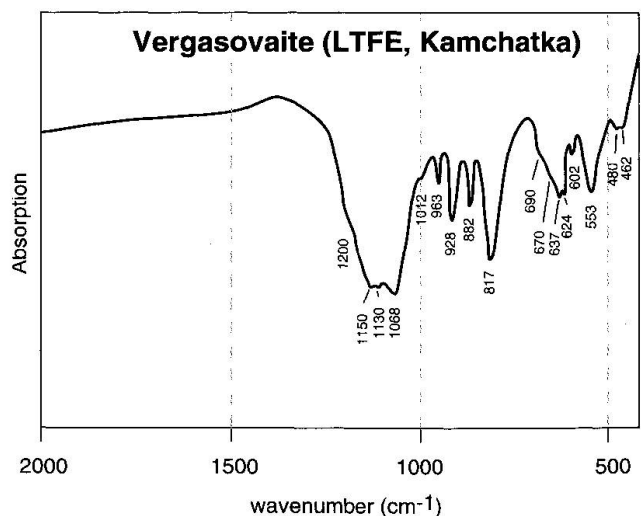


Fig. 5 IR-spectrum of vergasovaite. The new mineral is hydroxyl- and water-free.

Tab. 7 Chemical data for vergasovaite and Cu-bearing anglesite.

| Constituent                   | Wt%   | Range |       | Std. dev.<br>$\sigma_{n+1}$ | Probe Standard                    |
|-------------------------------|-------|-------|-------|-----------------------------|-----------------------------------|
|                               |       | Min   | Max   |                             |                                   |
| CuO                           | 49.81 | 47.88 | 52.35 | 1.17                        | Cu <sub>2</sub> O (synthetic)     |
| ZnO                           | 1.76  | 0.15  | 4.19  | 1.26                        | ZnSe (synthetic)                  |
| SO <sub>3</sub>               | 21.44 | 19.89 | 23.12 | 1.03                        | Ba[SO <sub>4</sub> ] (synthetic)  |
| MoO <sub>3</sub>              | 25.29 | 21.01 | 28.73 | 2.29                        | Ca[MoO <sub>4</sub> ] (synthetic) |
| V <sub>2</sub> O <sub>5</sub> | 0.88  | 0.10  | 1.81  | 0.59                        | vanadinite                        |
| PbO                           | 0.63  | 0.14  | 2.06  | 0.74                        | crocoite                          |
| Sum                           | 99.81 | 98.48 | 99.92 | 0.44                        |                                   |

Empirical formulae calculated on the basis of nine oxygens p.f.u. (EMP data).  
 N = 18 analyses for all constituents except for PbO (N = 6); acceleration voltage: 20 kV; beam current: 30 kV;  
 beam size: spot analyses.  
 A:  $(\text{Cu}_{2.82(7)}, \text{Zn}_{0.10(7)}, \text{Pb}_{0.01(1)})_{\Sigma = 2.91(9)} \text{O}[(\text{Mo}_{0.79(7)}, \text{S}_{0.20(5)}, \text{V}_{0.04(3)})_{\Sigma = 1.04(3)} \text{O}_4][\text{SO}_4]$   
 B:  $(\text{Cu}_{2.87(6)}, \text{Zn}_{0.06(2)})_{\Sigma = 2.92(6)} \text{O}[(\text{Mo}_{0.79(7)}, \text{S}_{0.21(7)}, \text{V}_{0.04(3)})_{\Sigma = 1.03(2)} \text{O}_4][\text{SO}_4]$

Formula derived from the crystal structure determination:  
 C:  $\text{Cu}_3\text{O}[(\text{Mo}_{0.742(7)}, \text{S}_{0.258(7)}) \text{O}_4][\text{SO}_4]$

Simplified formula:  
 D:  $\text{Cu}_3\text{O}[(\text{Mo,S})\text{O}_4][\text{SO}_4]$

A, D: this study; B, C, D: BERLEPSCH et al. (in press)

Two analyses of Cu-bearing anglesite (all wt%; same analytical conditions as for vergasovaite):  
 CuO: 2.10, 1.72; ZnO: n.d., 0.06; PbO: 70.83, 70.67;  
 SO<sub>3</sub>: 26.74, 27.37; V<sub>2</sub>O<sub>5</sub>: n.d., 0.01; Sum: 99.68, 99.83.  
 Empirical formula calculated on the basis of four oxygens p.f.u.:  $(\text{Pb}_{0.94}, \text{Cu}_{0.07})_{1.01} \text{S}_{1.00} \text{O}_4$

crystal structure determination and the previously obtained empirical formula  $(\text{Cu}_{2.87(6)}, \text{Zn}_{0.06(2)})_{\Sigma = 2.92(6)} \text{O}[(\text{Mo}_{0.79(7)}, \text{S}_{0.21(7)}, \text{V}_{0.04(3)})_{\Sigma = 1.03(2)} \text{O}_4][\text{SO}_4]$  (BERLEPSCH et al., in press). In all cases the simplified formula is  $\text{Cu}_3\text{O}[(\text{Mo,S})\text{O}_4][\text{SO}_4]$ .

Both set of analyses show good negative cor-

relations (Fig. 6; JEOL, N = 57, R = -0.84; CAMEBAX, N = 18, R = -0.73) between MoO<sub>3</sub> and SO<sub>3</sub> values (wt%) which indicates a considerable and unusual substitution of Mo<sup>6+</sup> by S<sup>6+</sup> (BERLEPSCH et al., in press). The Mo-S- and V-inhomogeneities can also be seen in the element distribution maps

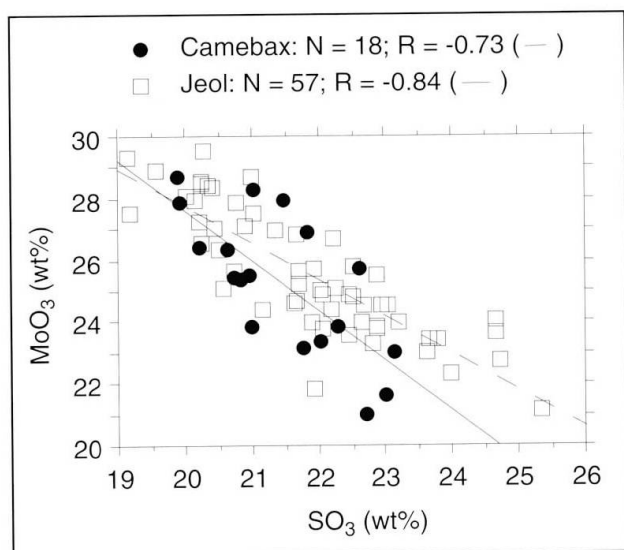


Fig. 6 Regression plot for MoO<sub>3</sub> wt% against SO<sub>3</sub> wt%. Vergasovaite displays an unusual substitution of S<sup>6+</sup> for Mo<sup>6+</sup> in the tetrahedral sites.

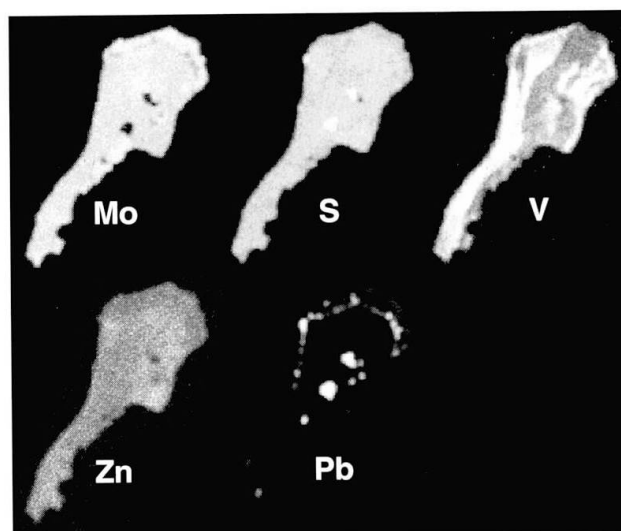


Fig. 7 Element distribution maps for vergasovaite to visualize sector and oscillatory zonation. Each map has an individual intensity scale which cannot be compared directly to the other ones.



Tab. 8 Transformation products of some anhydrous minerals after hydration and/or hydrolysis.

| a) hydration   |  |
|--|--|
| Tolbachite:  | Eriochalcite:  |
| $\text{CuCl}_2$  | $\rightarrow \text{CuCl}_2 \cdot 2 \text{H}_2\text{O}$   |
| Chloromagnesite:   | Bischofite:  |
| $\text{MgCl}_2$  | $\rightarrow \text{MgCl}_2 \cdot 6 \text{H}_2\text{O}$   |
| b) dissolution and re-deposition   |  |
| Piypite:   | Chalcantite + Mitscherlichite:   |
| $\text{K}_4\text{Cu}_4\text{O}_2[\text{SO}_4]_4 \cdot (\text{Na,Cu})\text{Cl}$ | $\rightarrow \text{Cu}[\text{SO}_4] \cdot 5 \text{H}_2\text{O} + \text{K}_2\text{CuCl}_4 \cdot 2 \text{H}_2\text{O}$ |
| Tenorite:  | Atacamite/paratacamite/<br>botallackite:   |
| $\text{CuO}$   | $\rightarrow \text{Cu}_2\text{Cl}(\text{OH})_3$  |

in figure 7. Note that the scales are relative ones and that the intensities cannot be compared directly from one element distribution map to another. In vergasovaite we observe both sector and oscillatory zonation, a phenomenon which is well known in crystals that grow rapidly, e.g., nabokoite  $\text{Cu}_7[\text{TeO}_4][\text{SO}_4]_5 \cdot \text{KCl}$  and atlasovite  $\text{Cu}_6\text{Fe}[\text{BiO}_4][\text{SO}_4]_5 \cdot \text{KCl}$  (both POPOVA et al., 1987). From figure 7 the important role of V in the sector zonation is clearly visible. In contrast to this, Mo and S (and Zn) cause the oscillatory zonation (cf. figure 4 too). Due to the distribution of anglesite inclusions in vergasovaite, we suppose Pb is involved in the oscillatory zonation too (Figs 4 and 7). To underline the unusual Pb  $\leftrightarrow$  Cu substitution, two analyses of Cu-bearing anglesite are listed in table 7 as well. The formula of Cu-bearing anglesite derived from the EMP data is  $(\text{Pb}_{0.94}, \text{Cu}_{0.07})\text{S}_{1.00}\text{O}_4$ .

### Chemically related compounds

Vergasovaite is isotypic with the fully oxidized synthetic Cu-molybdate  $\text{Cu}_3\text{O}[\text{MoO}_4]_2$  described by KIHLEBORG and NORRESTAM (1972) which has not previously been found in nature. In vergasovaite complete substitution of  $\text{S}^{6+}$  for  $\text{Mo}^{6+}$  reduces the average T2–O distance from 1.75 to 1.47 Å. The average distance T1–O in the mineral is 1.71 Å which agrees well with 26%  $\text{S}^{6+}$  substitution for  $\text{Mo}^{6+}$ . It is also striking that the Mo–O distances in the synthetic compound are 1.778 Å for T1 and 1.749 Å for T2. Thus the smaller site in the synthetic compound accepts a higher S substitution in the mineral (BERLEPSCH et al., in press).

Apart from this, vergasovaite  $\text{Cu}_3\text{O}[(\text{Mo,S})\text{O}_4][\text{SO}_4]$  is the first mineral which contains Cu, Mo, S, and O as its main elements, although several sul-

fates and molybdates of copper have been known for a long time. Among the 67 minerals containing Cu and  $\text{SO}_4$  as their main elements/element groups, only chalcocyanite  $\text{Cu}[\text{SO}_4]$  (WILDNER and GIESTER, 1988) and dolerophanite  $\text{Cu}_2\text{O}[\text{SO}_4]$  (EFFENBERGER, 1985) are  $\text{H}_2\text{O}$ - and hydroxyl-free sulfates of copper. Thus, an end-member compound  $\text{Cu}_3\text{O}[\text{SO}_4]_2$  is obviously not known. Several hydrated and/or hydroxylated sulfates of copper exist including antlerite  $\text{Cu}_3\text{SO}_4(\text{OH})_4$  (HAWTHORNE et al., 1989) which has the same space group and related lattice parameters as vergasovaite but a very different structure. Only five minerals are known which contain Cu and  $\text{MoO}_4$  as their main elements/element groups two of which are hydroxylated molybdates of copper: lindgrenite  $\text{Cu}_3[\text{MoO}_4]_2(\text{OH})_2$  (HAWTHORNE and EBY, 1985), and szenicsite  $\text{Cu}_3[\text{MoO}_4](\text{OH})_4$  (FRANCIS et al., 1994). As it is visible from the list presented by VERGASOVA and FILATOV (1993), hydrated and hydroxylated compounds of the LTFE result from hydration or by dissolution and redistribution due to interaction of meteoric waters with primarily anhydrous exhalates (Tab. 8).

### Conclusions

Many of the characteristic properties of vergasovaite are typical of the exhalative minerals found in the LTFE. As a direct consequence of the high-temperature formation of the exhalates,  $\text{H}_2\text{O}$ - and OH-free (anhydrous) minerals are abundant, i.e. chlorides, sulfates, arsenates, selenates and so on. The formation of hydrated and hydroxylated compounds was discussed in the previous section. Tolbachite  $\text{CuCl}_2$ , ponomarevite  $\text{K}_4\text{Cu}_4\text{OCl}_{10}$  and chalcocyanite  $\text{Cu}[\text{SO}_4]$  are typical indicators of anhydrous associations.

Due to the high temperatures and the presence of (atmospheric) oxygen, the LTFE exhalates are highly oxidized. Thus oxysalts, i.e. oxychlorides, oxysulfates, oxyselenates, are abundant and to these we now add the mixed oxymolybdate-sulfate vergasovaite. Furthermore, high oxidation states of the elements in the various minerals predominate:  $\text{Cu}^{2+}$ ,  $\text{Fe}^{3+}$ ,  $\text{V}^{5+}$ ,  $\text{As}^{5+}$ ,  $\text{Mo}^{6+}$ . Tenorite  $\text{CuO}$ , dolerophanite  $\text{Cu}_2\text{O}[\text{SO}_4]$  and melanothallite  $\text{Cu}_2\text{OCl}_2$  are also indicative of the oxidizing conditions.

Another characteristic feature of the LTFE minerals is related to the quickly changing conditions under which the minerals were formed. In fumaroles, there are distinct and frequent changes in temperature, pressure, redox-potential, and composition of the gas. Newly formed minerals

are highly dispersed and sector- and oscillatory zonation are as abundant as are many inclusions. Complex minerals from both the cationic and anionic point of view are characteristic for LTFE, i.e. arsenate-phosphates, chloride-vanadates, -sulfates, and sulfates-fluorides, sulfate-molybdates, oxy-selenate-chlorides, chloro-tellurate-sulfates and -bismuthate-sulfates in combination with Cu and with K, Na, Cs, Rb, Zn, Pb, Mg, Fe, Al, V.

The extreme concentration of certain elements, compared to the average concentrations in other rocks, is supposed to be related to a gradual accumulation of primarily rare elements. This is caused by both the exhalative activity and the interaction with exogenic factors. In particular, it is supposed that repeated cycles of precipitation, dissolution, infiltration, and re-precipitation led to the accumulation and finally to the observed high concentrations of particular elements. For instance the Mo-concentrations of 200–300 ppm in the exhalative Cu-ores are two orders of magnitude higher than the Clarke values for basic rocks: 1.4 ppm (VINOGRADOV, 1962); oceanic and upper crust: 0.8–1 ppm (TAYLOR and MCLENNAN, 1985); or basalts of oceanic islands: 2.4 ppm (SUN and MCDONOUGH, 1989). In addition, an increase of the Mo-concentrations in exhalative Cu-ores of the LTFE was observed within a very short period: from 240 ppm before 1980 (NABOKO and GLAVATSKIKH, 1983) up to 340 ppm in 1988 (NABOKO and GLAVATSKIKH, 1988). Such significant changes in concentrations cannot be explained solely by the change of composition of the gas, which is approximately constant for the short period indicated, but by a gradual accumulation as explained above.

Vergasovaite incorporates all these features: it is a rare, anhydrous, fully oxidized Cu-oxy-molybdate-sulfate with sector and oscillatory zonation that contains inclusions of Cu-bearing anglesite.

#### Acknowledgements

Our thanks are due to M. Kunz and T.M. Seward (both ETH Zürich) who carefully reviewed the manuscript. We appreciate the help of S. Graeser (Basel) in reference to the optical goniometer work and the indexation of the crystallographical faces. Our thanks are also due to M. Zehnder and M. Neuburger (both Basel) for the CAD4 measurements, to I.A. Bryzgalov and I.M. Kulikova (both Moscow) for providing the CAMEBAX EMP data and to N.V. Chukanov for performing the IR-spectrum.

#### References

- APPLEMAN, D.E. and EVANS, H.T.J. (1973): Job 9214: indexing and least squares refinement of powder diffraction data. Natl. Tech. Inf. Serv. U.S. Dep. Commerce, Springfield, Virginia, Document PB-216 188.
- BERLEPSCH, P., ARMBRUSTER, TH., BRUGGER, J., BYKOVA, E.Y. and KARTASHOV, P.M. (in press): The crystal structure of vergasovaite  $\text{Cu}_3\text{O}[(\text{Mo,S})\text{O}_4\text{SO}_4]$ , and its relation to synthetic  $\text{Cu}_3\text{O}[\text{MoO}_4]_2$  (Europ. J. Mineral.).
- BERNARD, A. and LE GUERN, F. (1986): Condensation of volatile elements in high-temperature gases of Mount St. Helens. *J. Volcanol. Geochem. Res.*, 28, 91–105.
- BERNARD, A., SYMONDS, R.B. and ROSE, W.I. (1990): Volatile transport and deposition of Mo, W, and Re in high-temperature magmatic fluids. *Appl. Geochem.*, 5, 317–326.
- BRAITSEVA, O.A., MELEKESTEV, I.V., PONOMAREVA, V.V. and SULERZHITSKY, L.D. (1995): Ages of calderas, large explosive craters and active volcanoes in the Kuril-Kamchatka region, Russia. *Bull. Volcanol.*, 57, 383–402.
- BYKOVA, E.Y., ZNAMENSKII, V.S., KOVALENKER, V.A., MARCEILLE, I.M. and BATURIN, S.B. (1995): Associations and conditions of formation of molybdenum minerals in exhalative products of Kudrjavii volcano, Iturup, Kurily island. *Geol. Ore Deposits*, 37/3, 265–273 (in Russian).
- DONNAY, J.D.H. and ONDIK, H.M. (1973): Crystal data determinative tables. 3rd ed. Vol. 2. U.S. Department of Commerce, National Bureau of Standards and the Joint Committee on Powder Diffraction Standards, USA.
- EFFENBERGER, H. (1985):  $\text{Cu}_2\text{O}(\text{SO}_4)$ , dolerophanite: refinement of the crystal structure, with comparison of  $[\text{OCu}(\text{II})_4]$  tetrahedra in inorganic compounds. *Monatshfte für Chemie*, 116, 927–931.
- FEDOTOV, S.A. and MARKHININ, Y.K. (1984): The great Tolbachik fissure eruption: geological and geophysical data 1975–1976 (Cambridge Earth Sciences Series), XII. Cambridge University Press, Cambridge, 341 pp.
- FRANCIS, C.A., PITMAN, L.C. and LANGE, D.E. (1994): Szencsite, a new mineral from Tierra Amarilla, Chile. *Mineral. Rec.*, 25, 76.
- HAWTHORNE, F.C. and EBY, R.K. (1985): Refinement of the crystals-structure of lindgrenite. *N. Jb. Mineral. Mh.*, 1985, 234–240.
- HAWTHORNE, F.C., GROAT, L.A. and EBY, R.K. (1989): Antlerite,  $\text{Cu}_3\text{SO}_4(\text{OH})_4$ , a heteropolyhedral wall-paper structure. *Canad. Mineral.*, 27, 205–209.
- KAVALIERS, I. (1994): High Au, Ag, Mo, Pb, V, and W content of fumarolic deposits at Merapi volcano, Central Java, Indonesia. *J. Geochem. Explor.*, 50, 479–491.
- KIHLBORG, L. and NORRESTAM, R. (1972): The symmetry of  $\text{Cu}_3\text{Mo}_2\text{O}_9$ . *Acta Cryst.*, B28, 3097.
- MANDARINO, J.A. (1979): The Gladstone-Dale relationship, part III: some general applications. *Canad. Mineral.*, 17, 71–76.
- MANDARINO, J.A. (1981): The Gladstone-Dale relationship, part IV: the compatibility concept and its application. *Canad. Mineral.*, 19, 441–450.
- NABOKO, S.I. and GLAVATSKIKH, S.F. (1983): Post eruptive metasomatose and ore formation. *Nauka, Moscow*, 168 pp. (in Russian).
- NABOKO, S.I. and GLAVATSKIKH, S.F. (1988): Evolution of post eruptive metasomatism and ore mineral genesis on cones of the Large Tolbachik Fissure Eruption

- (LTFE, 1975–1986). *Volcanology and Seismology*, 1, 56–69 (in Russian).
- POPOVA, V.I., POPOV, RUDASHEVSKIY, N.S., GLAVATSKIKH, S.F., POLYAKOV, V.O. and BUSHMAKIN, A.F. (1987): Nabokoite  $\text{Cu}_7\text{TeO}_4(\text{SO}_4)_5 \cdot \text{KCl}$  and atlasovite  $\text{Cu}_6\text{Fe}^{3+}\text{Bi}^{3+}\text{O}_4(\text{SO}_4)_5 \cdot \text{KCl}$ . New minerals of volcanic exhalations. *Zapiski Vses. Mineralog. Obshch.*, 116, 358–367 (in Russian).
- SUN, S.S. and McDONOUGH, W.F. (1989): Chemical and isotopic systematics of the oceanic basalts; implications for mantle composition and processes. In: SAUNDERS, A.D. and NORRY, M.J. (eds): *Magmatism in the ocean basins*. *Geol. Soc. Proc. Pub.* 42, 313–345.
- TAYLOR, S.R. and MCLENNAN, S.M. (1985): *The continental crust: its composition and evolution. An examination of the geochemical record preserved in sedimentary rocks*. Blackwell Scientific Publications, Oxford and Palo Alto, xvi + 312 pp.
- VERGASOVA, L.P. and FILATOV, S.K. (1993): Minerals of volcanic exhalations – a new genetic group (after the data of Tolbachik volcano eruption in 1975–1976). *Proc. Rus. Mineral. Soc.*, 122/4, 68–76 (in Russian).
- VINOGRADOV, A.P. (1962): Average contents of chemical elements in the principal types of igneous rocks of the Earth's crust. *Geochemistry*, 1962/7, 641–664.
- WILDNER, M. and GIESTER, G. (1988): Crystal structure refinement of synthetic chalcocyanite ( $\text{CuSO}_4$ ) and zincosite ( $\text{ZnSO}_4$ ). *Mineral. Petrol.*, 39, 201–209.
- YVON, K., JEITSCHKO, W. and PARTHÉ, E. (1997): LAZY PULVERIX, a computer program, for calculating X-ray and neutron diffraction powder patterns. *J. Appl. Crystallogr.*, 10, 73–74.
- ZAMBONINI, F. (1935): *Mineralogia Vesuviana*. Napoli, 455 pp.

Manuscript received May 14, 1998; revision accepted August 12, 1998.